Journal of Materials Science & Technology 33 (2017) 751–757

Contents lists available at ScienceDirect

Journal of Materials Science & Technology

journal homepage: www.jmst.org

Formation, Structures and Electronic Properties of Silicene Oxides on Ag(111)

Muhammad Ali [1], Zhenyi Ni [1], Stefaan Cottenier [2], Yong Liu [1], Xiaodong Pi [1,*], Deren Yang [1]

[1] State Key Laboratory of Silicon Materials and School of Materials Science and Engineering, Zhejiang University, Hangzhou 310027, China
[2] Center for Molecular Modeling (CMM) and Department of Materials Science and Engineering (DMSE), Ghent University, Zwijnaarde BE-9052, Belgium

ARTICLE INFO

Article history:
Received 13 May 2016
Received in revised form 3 August 2016
Accepted 19 August 2016
Available online 25 August 2016

Key words:
Silicene oxides
Ag(111)
Density functional theory
Oxidation
Hybridization
Band gap

ABSTRACT

The formation, structural and electronic properties of silicene oxides (SOs) that result from the oxidation of silicene on Ag(111) surface have been investigated in the framework of density functional theory (DFT). It is found that the honeycomb lattice of silicene on the Ag(111) surface changes after the oxidation. SOs are strongly hybridized with the Ag(111) surface so that they possess metallic band structures. Charge accumulation between SOs and the Ag(111) surface indicates strong chemical bonding, which dramatically affects the electronic properties of SOs. When SOs are peeled off the Ag(111) surface, however, they may become semiconductors.

1. Introduction

The pronounced relativistic effects of silicene, the graphene equivalent of silicon, have recently attracted great attention and opened a new door to the next generation silicon technology[1–8]. It is well known that spin–orbit coupling in silicene is stronger than that in graphene, making silicene a promising candidate for topological insulators[9]. In contrast to graphene, sp^3 hybridized low-buckled silicene cannot be exfoliated from bulk silicon. Thus, supporting substrates are needed for the growth of silicene. Up to now silicene is often epitaxially grown on metallic substrates. Among all the metallic substrates, Ag(111) is the most popular because of the good lattice match between silicene and Ag(111). For silicene on Ag(111) a metallic band structure has been observed by using angle resolved photoemission spectroscopy (ARPES)[10]. Density functional theory (DFT) calculations have shown that strong coupling between Si *p* states and Ag *d* states is critical to the formation of the metallic band structure of silicene[11,12]. The metallic behavior of silicene on Ag(111) is a key barrier to the practical use of silicene in device applications.

Oxidation is known to be vital for the tuning of the properties of two-dimensional layered materials. For example, the oxidation of freestanding silicene can cause silicene to change from a semimetal to a semiconductor[13]. It has been observed that controlled oxidation may significantly alter the electronic properties of silicene on Ag(111)[14–16]. Band gaps have been indicated for silicene oxides (SOs) on Ag(111) by scanning tunneling microscopy (STM)[15]. However, the *sp* band of Ag crossing the Fermi level in ARPES measurements and calculated density of states (DOS) have shown the absence of the band gap opening for SOs on Ag(111)[16]. Recent ARPES measurements supported by X-ray adsorption spectroscopy (XAS) and X-ray emission spectroscopy (XES) have further demonstrated that SOs on Ag(111) do not have band gaps[17]. It is clear that SOs on Ag (111) should be systematically studied to render a consistent picture on their properties.

In this work a variety of SOs with the charge states of Si from +1 to +4 on three slabs of Ag(111) facet have been modeled in the framework of DFT. The formation, structures and electronic properties of all the SOs on Ag(111) are analyzed. It is found that the honeycomb structure of silicene on Ag(111) is highly distorted after oxidation. SOs interact with the underlying Ag(111) substrate, leading to the metallic nature of SOs. However, tunable band gaps may be obtained for SOs after they are peeled off Ag(111).

2. Computational Methods

The first-principles calculations of SOs on Ag(111) were performed by using the Vienna *Ab-initio* Simulation Package (VASP)

* Corresponding author.
E-mail address: xdpi@zju.edu.cn (X. Pi).

http://dx.doi.org/10.1016/j.jmst.2016.08.020
1005-0302/

with the projected-augmented wave (PAW) method[18–20]. The Perdew–Burke–Ernzerhof (PBE) correlation exchange functional at the generalized gradient approximation (GGA) was employed. The valence electron wave functions were expanded using a plane wave basis set with a cutoff kinetic energy of 400 eV[21]. The geometry optimization was performed with a conjugate-gradient algorithm. All the atoms were relaxed into their ground states until changes in the energy and remaining force for all the atoms became less than 1×10^{-5} eV and 0.01 eV/Å, respectively. In the geometry optimization and the calculation of densities of states (DOS) the two-dimensional Brillouin zone was sampled using Γ-centered $(3 \times 3 \times 1)$ and $(5 \times 5 \times 1)$ Monkhorst–Pack k-point grids, respectively[3,22]. The Ag(111) substrate was modeled by adopting a slab model consisting of three layer atoms cleaved from the face-centered cubic (*fcc*) Ag with a lattice constant of 4.09 Å. A 30 Å wide vacuum layer was introduced in the z-direction to eliminate the interaction between periodic images. The charge redistribution between SOs and Ag(111) was analyzed by means of Bader charge calculations[23,24]. Please note that the van der Waals (vdW) interaction between SOs and Ag(111) was not considered in our calculations because covalency plays a major role in the interaction between Si and Ag states[25–28].

3. Results and Discussion

3.1. Structures of silicene oxides on Ag(111)

A 4×4 silicene superstructure on Ag(111) is currently the most typical silicene structure because it is often grown as a single phase with a larger area than other silicene superstructures on Ag(111). All silicene superstructures are metallic due to strong coupling between Ag *4d* states and Si *3p* states[11,27,28]. Therefore, the 4×4 silicene superstructure on Ag(111) is chosen to representatively investigate the oxidation of silicene on Ag(111). Fig. 1 shows the optimized structures of the original and oxidized 4×4 silicene on Ag(111) with both side and top views. All kinds of oxygen configurations in SOs have been considered. They are denoted as O_{qb}, O_{db}, O_{ob}^{d}, O_{ob}^{sT} and O_{ob}^{sB}, which are defined in the caption of Fig. 1. It is seen in Fig. 1(a) that the Si—Si bond lengths of silicene are 2.28–2.37 Å. The buckling distance is 0.77 Å. Since an O_{qb} atom takes the position between two neighboring Si atoms to form a Si—O—Si bond, all the silicon atoms become three-fold coordinated with oxygen for the SO with O_{qb}. The original honeycomb ring of six silicon atoms transforms to a larger twelve-atom ring, as shown in Fig. 1(b). However, the buckling between silicon and oxygen atoms in SO with O_{qb}

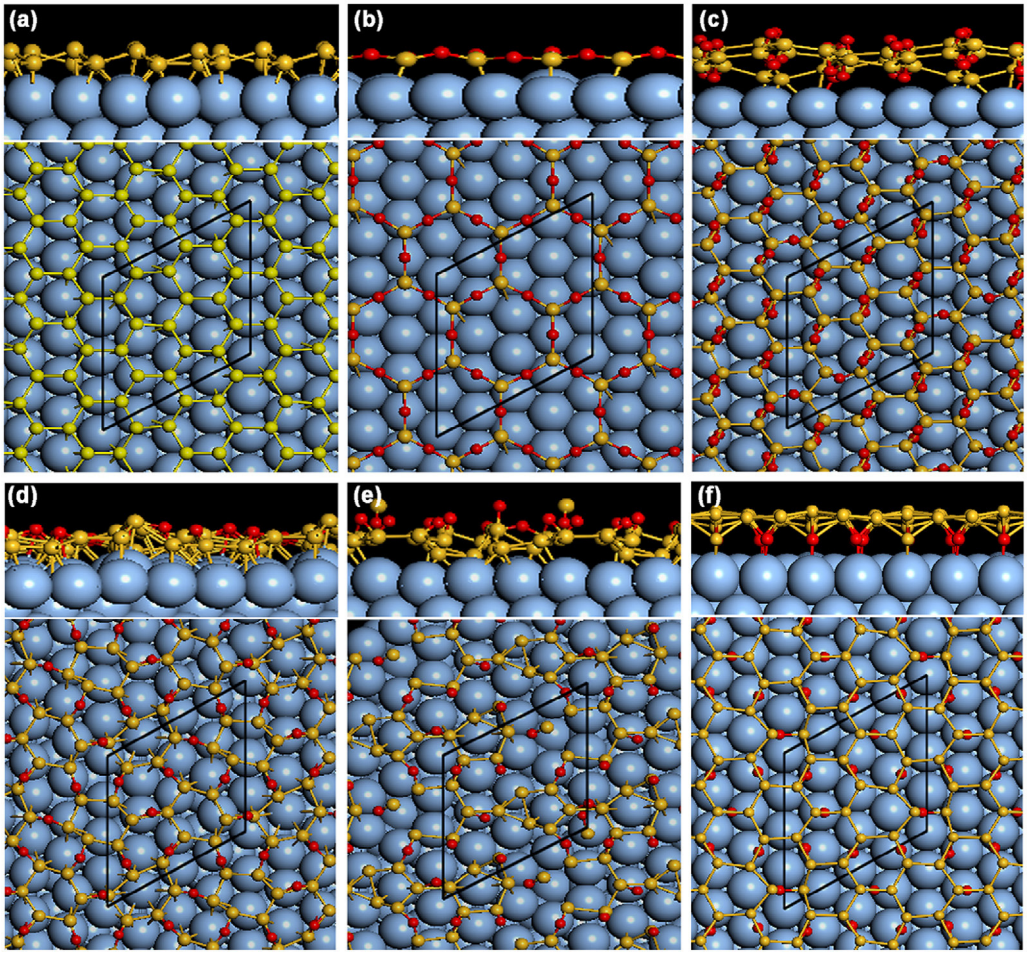

Fig. 1. Atomic structures of silicene and silicene oxides on Ag (111). (a) 3×3 silicene. 3×3 silicene oxides with (b) O_{qb} (an O atom bridges two neighboring Si atoms), (c) O_{db} (two O atoms oxidize each Si—Si bond at only one pair of opposite sides in a hexagonal ring), (d) O_{ob}^{d} (an O atom overbridges two Si atoms at both sides of silicene), (e) O_{ob}^{sT}(an O atom overbridges two Si atoms only at the top side of silicene), (f) O_{ob}^{sB} (an O atom overbridges two Si atoms only at the bottom side of silicene). Red, yellow and blue balls represent oxygen, silicon and silver atoms, respectively.

is similar to that of the original structure of silicene. The O—Si—O and Si—O—Si bond angles are 114.6° and 161.1°, respectively. The Si—O bond lengths (1.75–1.88 Å) are slightly larger than that in silica. Fig. 1(c) shows the double bridging of oxygen in the SO with O_{db}. Si—Si bonds at only one pair of opposite sides in a hexagonal lattice are oxidized. O_{db} leads to symmetric Si—O—Si bonds with respect to the oxidation-flatted plane of Si atoms. It is noticed that the incorporation of O_{db} distorts the honeycomb lattice of silicene. The distortion of honeycomb lattice increases the Si—Si bond length from 2.28 to 2.37 Å. The bond angles of Si—Si—Si and Si—O—Si vary from 106.59° to 120.17° and 89.11° to 92.04°, respectively. In this configuration, an sp^3 hybridized silicon atom is four-fold coordinated with two oxygen atoms and two silicon atoms. The resulting saturation of dangling bonds is advantageous for the stabilization of silicene. In Fig. 1(d) each O atom overbridges two neighboring Si atoms through their unpaired electrons. Such kind of overbridging O atoms can be found at either both sides (O^d_{ob}) or single side (O^{sT}_{ob} and O^{sB}_{ob}) of silicene. It is noticed that the honeycomb lattice of silicene is distorted to a certain extent after the incorporation of O^d_{ob} in silicene on Ag(111). The bond lengths are compressed up to 2.17 Å and the bond angles are either stretched or compressed after the oxidation of double sides. In contrast to O^d_{ob}, the top-side-only oxidation induced O^{sT}_{ob} severely distorts the honeycomb structure of silicene, as shown in Fig. 1(e). All the Si—Si bond lengths are either stretched or compressed in the SO with O^{sT}_{ob}. When oxidation takes place only at the bottom side of silicene i.e., between silicene and Ag(111), the honeycomb lattice of silicene remains in the original shape, as shown in Fig. 1(f). The Si—Si bond lengths in the SO with O^{sB}_{ob} are similar to that in the original epitaxial silicene on Ag(111). Both sp^2 and sp^3 hybridizations of Si are observed in the SO with O^{sB}_{ob}.

The charge states of Si in SOs with O_{qb}, O_{db}, O^d_{ob}, O^{sT}_{ob} and O^{sB}_{ob} are +3, +2, +1, +1 and +1, respectively. SOs with O_{qb}, O_{db}, O^d_{ob}, O^{sT}_{ob} and O^{sB}_{ob} are actually partially oxidized silicene because all the charge states of Si are smaller than +4. For the full oxidation of silicene, O_{qb} should be integrated with O^d_{ob}, O^{sT}_{ob}, and O^{sB}_{ob} to achieve the charge state of +4 for Si. However, the optimized structures of fully oxidized silicene are found to be discontinuous (Fig. S1 in the Supporting Information). Therefore, the structures of fully oxidized silicene on Ag(111) are not further investigated in the current work.

We consider that SOs result from the reaction between silicene and molecular oxygen. In an oxygen atmosphere with the temperature of T and pressure of p, the surface free energy $\gamma(T, p)$ of a specific SO can be calculated by using

$$\gamma(T, p) = \frac{1}{A}[G(T, p, N_{Ag}, N_{Si}, N_O) - N_{Ag}\mu_{Ag}(T, p) - N_{Si}\mu_{Si}(T, p) - N_O\mu_O(T, p)], \quad (1)$$

where $G(T, p, N_{Ag}, N_{Si}, N_O)$ is the Gibbs free energy of the SO with the area of A. N_{Ag}, N_{Si} and N_O are the numbers of Ag, Si and O atoms, respectively. μ_{Ag}, μ_{Si}, and μ_O are the chemical potentials of Ag, Si and O, respectively. The Gibbs free energy for a solid phase may be obtained by using

$$G = E_{tot} + F_{conf} + F_{vib} + PV, \quad (2)$$

where E_{tot} is the total electronic energy. F_{conf} and F_{vib} are the configurational and vibrational free energies, respectively. P and V are pressure and volume of the unit cell, respectively. According to previous studies[29,30], F_{conf}, F_{vib} and PV are rather small compared with E_{tot}. Therefore, G can be approximated by E_{tot}. In addition, μ_O may be calculated by using

$$\mu_O(T, p) = \frac{1}{2}\left[E^{tot}_{O_2} + \tilde{\mu}_{O_2}(T, p^o) + k_B T \ln\left(\frac{p}{p^o}\right)\right], \quad (3)$$

where $E^{tot}_{O_2}$ is the total energy of an isolated O_2 molecule. $\tilde{\mu}_{O_2}(T, p^o)$ is the standard chemical potential of oxygen gas reported in the JANAF thermodynamics table[31]. p^o is equal to 1.01×10^5 Pa. k_B is the Boltzmann constant. The chemicalpotentials μ_{Ag} and μ_{Si} are

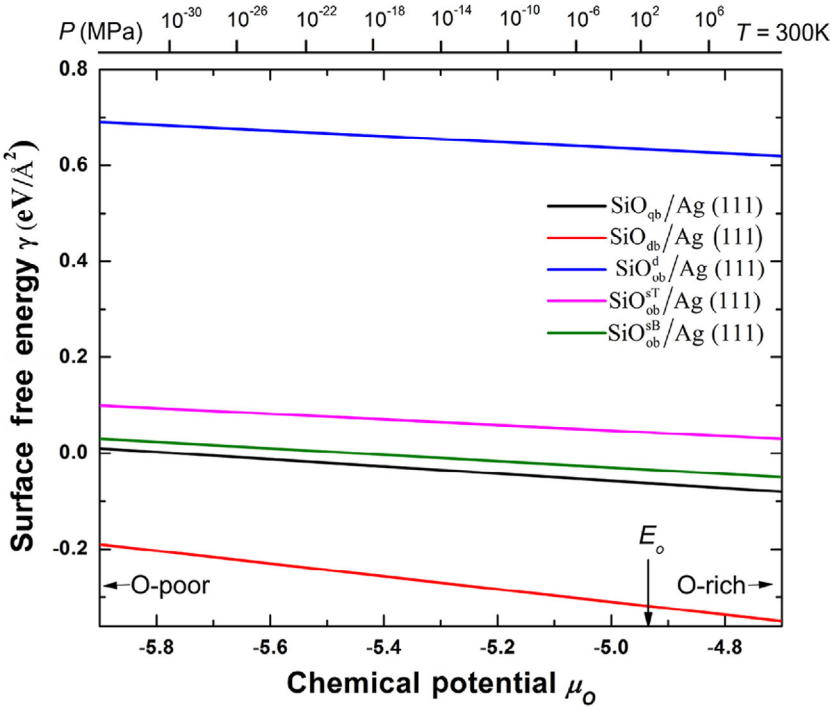

Fig. 2. Surface free energy (γ) as a function of oxygen chemical potential (μ_O) or oxygen pressure at 300 K. The total energy of one oxygen atom in an isolated molecule is indicated by the arrow.

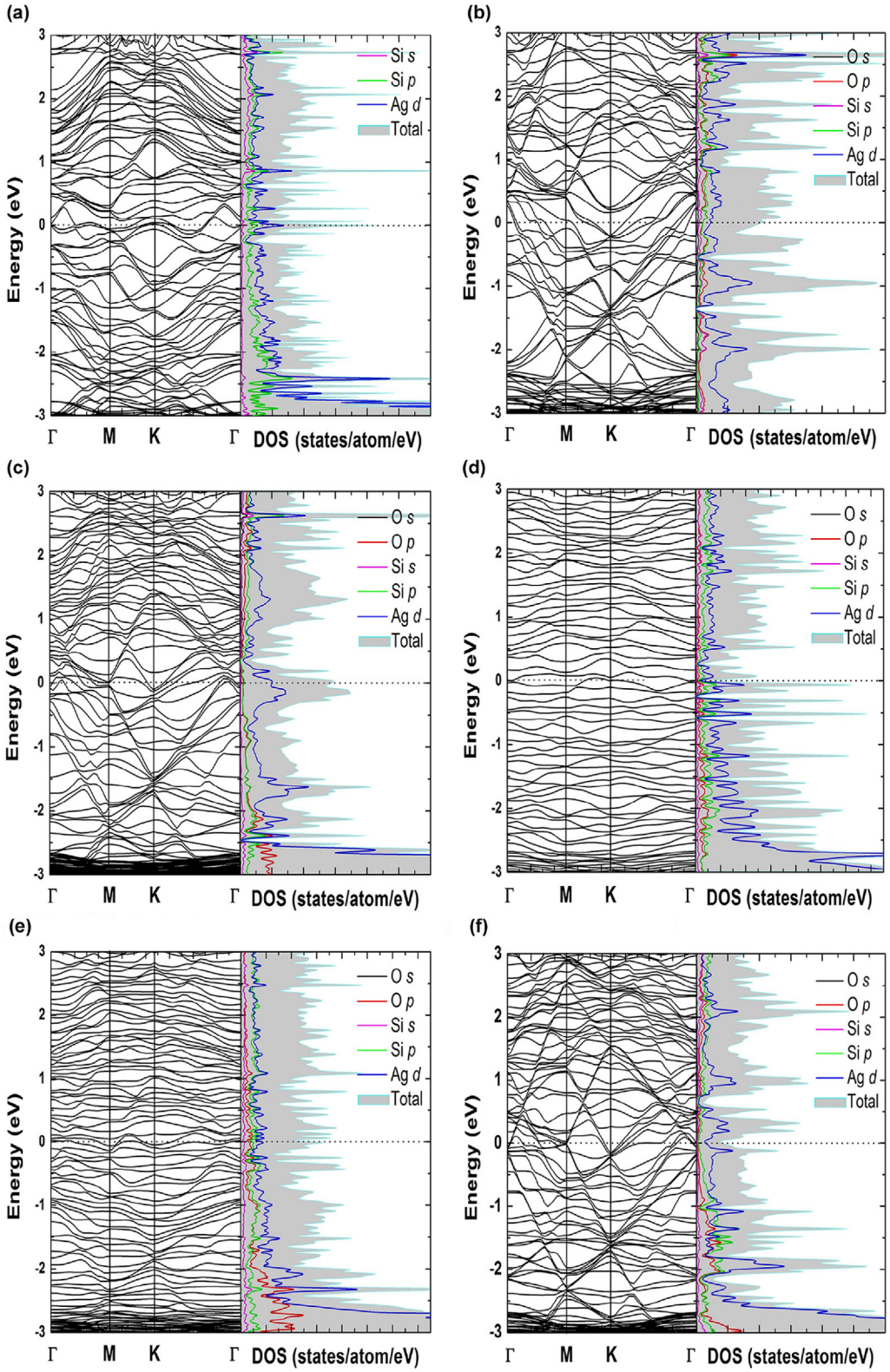

Fig. 3. Band structures and density of states of (a) silicene, silicene oxides with (b) O_{qb}, (c) O_{db}, (d) O^{d}_{ob}, (e) O^{sT}_{ob}, (f) O^{sB}_{ob} on Ag(111), respectively.

determined by dividing the total energies of Ag and Si unit cells by the number of atoms in the unit cells[32].

Fig. 2 shows the surface free energy of SOs on Ag(111) as a function of μ_{O_2}. We have converted μ_{O_2} to a pressure scale at 300 K byusing Eq. (3) in order to facilitate comparison with experiments. In general, the surface free energy of each SO decreases as μ_{O_2} increases. This means that the surface free energy has negative slope for SOs, indicating that the formation of SOs becomes more favorable in the abundance of oxygen gas. It is clear that the surface free energy decreases in the sequence of SOs with O^{d}_{ob}, O^{sT}_{ob}, O^{sB}_{ob}, O_{qb} and O_{db}. Since the SO with O_{db} has the lowest surface free energy, the SO with O_{db} can be the most likely produced during the

oxidation of silicene in the atmosphere of oxygen gas. In contrast, the SO with O^{d}_{ob} is the most unlikely formed given its largest surface free energy among all the SOs.

3.2. Electronic properties

Fig. 3 shows the band structures and the partial densities of states (PDOSs) of silicene and SOs on Ag(111). For silicene the Si *p* states and the Ag *d* states cross the Fermi level, indicating the metallic nature of silicene on Ag(111) (Fig. 3(a)). The interaction between silicene and Ag(111) is a central issue in the silicene research. It is well known that silicene is less stable and highly reactive than graphene because of its out-of-plane dangling bonds. When silicene is synthesized on Ag(111), these out-of-plane dangling bonds ($3p_z$ orbitals) of Si atoms are saturated by forming chemical bonds with the 4*d* electrons of Ag. Such coupling between Si and Ag induces symmetry breaking. The electronic bands around the Fermi level primarily originate from the hybridized 3*p* orbitals of Si and 4*d* orbitals of Ag, as shown in Fig. 3(a). The strong hybridization between Si and Ag orbitals results in a surface metallic band and the loss of the Dirac fermion characteristics in silicene on Ag(111). The Si *s* states predominantly contribute to the lowest lying states of the valence band, leading to σ bonding. The highest region of the valence band and the lowest region of the conduction band are primarily derived from the Si *p* states and Ag *d* states. Moreover the vertical spacing between the lower Si atoms and the topmost Ag atoms (2.14 Å), and the atomic radii of Si (1.18 Å) and Ag (1.65 Å) confirm the covalent bonding between Si and Ag. It is seen in the previous studies that the van der Waals (vdW) force has no influence on the modification of electronic properties because of the covalency between Si and Ag[25–28]. In case of SOs with O_{qb} the Fermi level is located in the conduction band with strong hybridization between Si *p* and O *p* states in both valence and conduction bands, as shown in Fig. 3(b). The strong contributions of the Si *s* and *p* states, O *p* states and Ag *d* states across the Fermi level lead to the formation of a metallic band structure. In case of SO with O_{db} the two Si—O—Si bonds at only one pair of opposite sides in a hexagonal lattice of silicene remarkably mitigate the interaction between Si and Ag states, as shown in Fig. 3(c). But the metallic substrate still has greater influence on the band hybridization, leading to a metallic band structure. The PDOS of SO with O_{db} demonstrates strong coupling between Si *p* and O *p* states throughout the valence and conduction bands. In both cases of SOs with +3 and +2 charge states of Si, the PDOSs have shown a strong resonance between Si *p* and O *p* states instead of Si *p* and Ag *d* states. In the cases of SOs with O^{d}_{ob} and O^{sT}_{ob} there are strong contributions of the Si *s*, Si *p* and Ag *d* states spanning the Fermi level, as shown in Fig. 3(d and e). Hence, no band gap is induced in both of the SOs. It is noticed that the strong hybridization between Si and Ag states is considerably decoupled at the Fermi level by the incorporation of O^{sB}_{ob} in silicene, as shown in Fig. 3(f). But it could not open a band gap in the silicene on Ag(111), either.

All the PDOS plots suggest that the overlapping of oxygen and Ag(111) enables the re-arrangement of electrons, leading to the chemisorption between SOs and Ag(111)[33]. It is evident that SOs with all oxidation states do not possess band gaps because the strong hybridization effects promote the metallic character of SOs on Ag(111). Our results are consistent with those obtained by Xu et al. and Johnson et al.[16,17]. Please note that XAS and XES studies have recently confirmed the metallic nature of SOs on Ag(111)[17].

The interface interaction plays a vital role in modulating the electronic properties of silicene on Ag(111). In order to probe the interface interaction, the charge density differences may be obtained by subtracting the charge densities of isolated SOs and Ag(111) from the total charge density of the hybrid structures, as shown in Fig. 4. It is clearly seen that the charge depletes from Si atoms and accumulates at the interfaces between SOs and Ag(111). The yellow (cyan) color represents the excess (deficit) of electrons at an interface region. The yellow lobes indicate strong bonding between Si and Ag atoms in all the SOs except for SO with O^{sB}_{ob}.

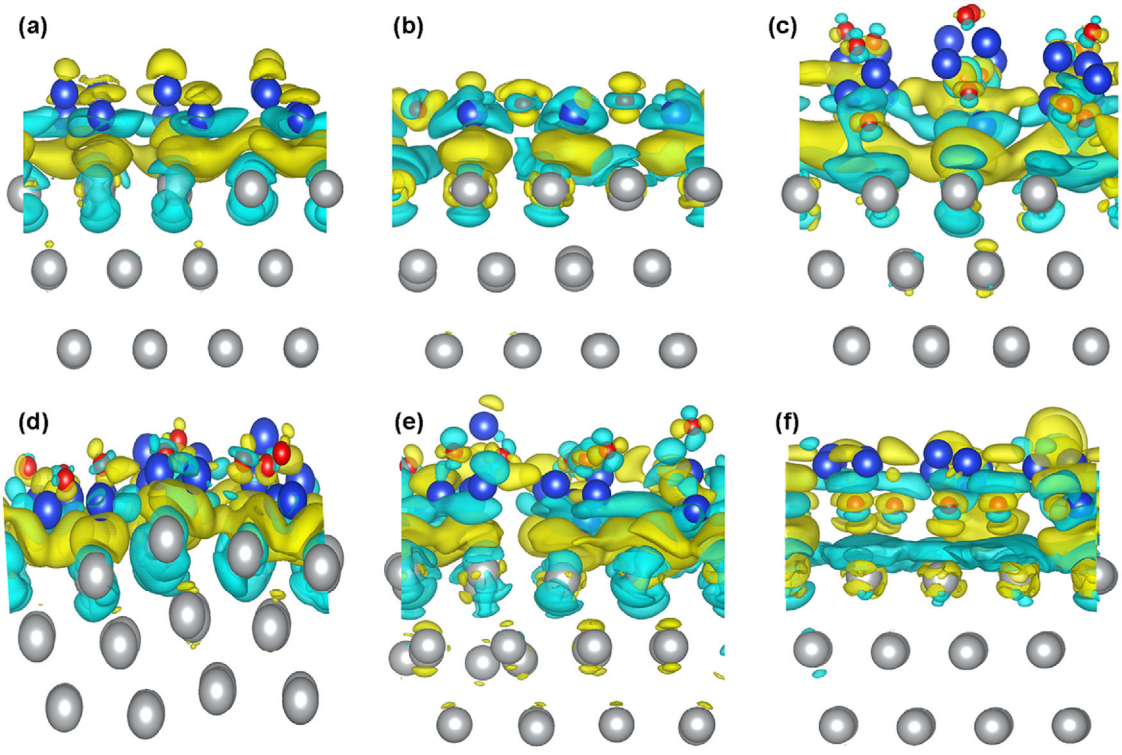

Fig. 4. Charge density differences for (a) silicene and silicene oxides with (b) O_{qb}, (c) O_{db}, (d) O^{d}_{ob}, (e) O^{sT}_{ob}, (f) O^{sB}_{ob} on Ag(111). Red, blue and gray balls are oxygen, silicon and silver atoms, respectively. The yellow and cyan colors indicate charge accumulation and depletion, respectively.

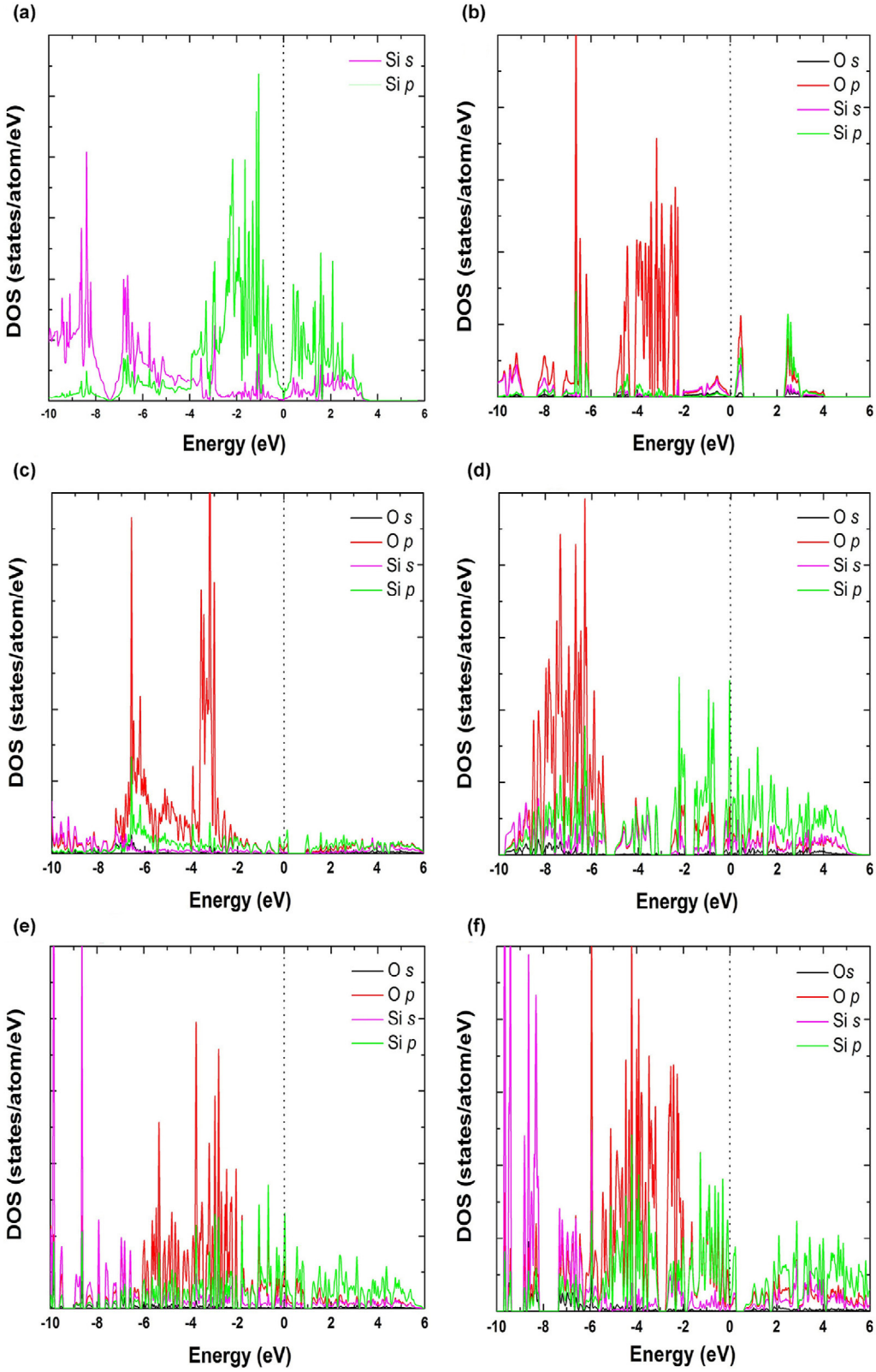

Fig. 5. Partial density of states (PDOS) of (a) silicene, silicene oxides with (b) O_{qb}, (c) O_{db}, (d) O^{d}_{ob}, (e) O^{sT}_{ob} and (f) O^{sB}_{ob}. All the structures are peeled off Ag(111).

In case of SO with O^{sB}_{ob}, there is week bonding between Si and Ag atoms because of the presence of O atoms between them, as shown in Fig. 4(f). To further probe the charge distribution between silicene/SOs and Ag(111), Bader charge calculations are performed. According to Bader charge analysis, the epitaxial silicene donates 0.62 electrons to Ag(111) because the Pauling electronegativity of Ag is slightly higher than that of Si. This is consistent with previous findings[21,34]. The Pauling electronegativities of O, Si and Ag are 3.44, 1.90 and 1.93, respectively[35]. Among all the elements O is the most electronegative, causing charge transfer from Ag(111) to SOs except for the SO with O^{sT}_{ob}. The exact amount of transferred charge is shown in Table 1. It is found that 0.45e transfers from the

Table 1
Structural properties of silicene oxides on Ag(111)

Configuration	Formula	Charge state of Si	Si—Si (Å)	Si—O (Å)	∠Si—Si—Si	∠Si—O—Si	Charge transfer (e)
SiO_{qb}	Si_6O_9	+3		1.75–1.87		161.13	0.32[a]
SiO_{db}	$Si_{18}O_{18}$	+2	2.28–2.37	1.61–1.75	106.58–120.17	89.11–92.04	0.74[a]
SiO^{d}_{ob}	$Si_{18}O_9$	+1	2.17–2.28	1.39–1.69	91.77–130.58	119.12–147.49	0.64[a]
SiO^{sT}_{ob}	$Si_{18}O_9$	+1	2.19–2.41	1.47–1.72	109.62–114.27	81.75–126.95	0.45[b]
SiO^{sB}_{ob}	$Si_{18}O_9$	+1	2.23–2.34	1.72–1.78	108.13–123.70	80.48	1.53[a]

[a] Charge was transferred from Ag(111) to SO.
[b] Charge was transferred from SO to Ag(111).

SO with O^{sT}_{ob} to Ag(111). This should be due to the fact that O atoms are separated from Ag atoms by Si atoms in the SO with O^{sT}_{ob}.

We have examined the PDOS of silicene and SOs after they are peeled off Ag(111). The electronic structures of peeled-off silicene and SOs are remarkably different from those of optimized ones on Ag(111), as shown in Fig. 5. The peeled-off silicene retrieves its semi-metallic characteristic. In the peeled-off SOs the buckling patterns of silicon and oxygen atoms are different from that of freestanding silicene. This indicates that the complex buckled geometries in the peeled-off SOs give rise to complex rehybridization between the *p* orbitals of Si and O atoms. If we assume that the zero-DOS region near the Fermi level is a band gap, the peeled-off SOs with O_{qb}, O_{db}, O^{d}_{ob} and O^{sB}_{ob} would have the band gaps of 2.31, 0.71, 0.29 and 0.28 eV, respectively (Fig. 5(b–d and f)). It is the presence of Ag(111) that makes the SOs metallic. Please note that the peeled-off SO with O^{sT}_{ob} remains metallic. Such a metallic behavior of the SO with O^{sT}_{ob} may be due to the fact that the original honeycomb structure is distorted to certain extent after oxidation. In case of the SO with O_{qb} there are localized states in the band gap. These localized states mainly originate from the Si *s*, *p* and O *p* states. Our Bader charge analysis indicates that polar bonds are formed between Si and O atoms. The electron density around O is higher than that around Si because the electronegativity of O is higher than that of Si. The peaks in PDOS correspond to the distinctive character of covalent bonding between silicon and oxygen atoms[36]. We should mention that the semiconducting SOs may be experimentally realized by etching the Ag(111) substrate, similar to what have been recently done for silicene[7].

4. Conclusion

Our first-principles calculations have shown that a variety of SOs on Ag(111) may be produced by the oxidation of epitaxial silicene. It is found that the honeycomb lattice of silicene changes to a certain extent after oxidation. SOs are strongly hybridized with the Ag(111) surface so that SOs have metallic band structures. Oxidation cannot completely eliminate the strong interface interaction between silicene and Ag(111). Charge transfer between SOs and Ag(111) indicates strong chemical bonding between Si and Ag atoms. The resulting strong interaction between SOs and Ag(111) dramatically affects the electronic properties of SOs. However, SOs may possess semiconducting characteristics after peeling off the Ag(111).

Acknowledgments

This work was supported by the National Basic Research Program of China (Grant No. 2013CB632101), the National Natural Science Foundation of China (Grant Nos. 61222404 and 61474097) and the Program of the Ministry of Education of China for Innovative Research Teams in Universities (Grant No. IRT13R54).

Appendix. Supplementary material

Supplementary data to this article can be found online at doi:10.1016/j.jmst.2016.08.020.

References

[1] A. Fleurence, R. Friedlein, T. Ozaki, H. Kawai, Y. Wang, Y. Yamada-Takamura, Phys. Rev. Lett 1 (2012) 108.
[2] L. Meng, Y. Wang, L. Zhang, S. Du, R. Wu, L. Li, Y. Zhang, G. Li, H. Zhou, W. Hofer, Nano Lett 13 (2013) 685.
[3] P. Vogt, P. De Padova, C. Quaresima, J. Avila, E. Frantzeskakis, M.C. Asensio, A. Resta, B. Ealet, Phys. Rev. Lett 108 (2012) 155501.
[4] L. Chen, C.C. Liu, B. Feng, X. He, P. Cheng, Z. Ding, S. Meng, Y. Yao, K. Wu, Phys. Rev. Lett 109 (2012) 056804.
[5] S. Cahangirov, M. Topsakal, E. Akturk, H. Sahin, S. Ciraci, Phys. Rev. Lett 102 (2009) 236804.
[6] Q. Tang, Z. Zhou, Prog. Mater. Sci. 58 (2013) 1244.
[7] L. Tao, E. Cinquanta, D. Chiappe, C. Grazianetti, M. Fanciulli, M. Dubey, A. Molle, D. Akinwande, Nat. Nanotechnol. 10 (2015) 227.
[8] R. Wang, M.S. Xu, X.D. Pi, Chin. Phys. B 24 (2015) 086807.
[9] C.C. Liu, W. Feng, Y. Yao, Phys. Rev. Lett. 107 (2011) 076802.
[10] D. Tsoutsou, E. Xenogiannopoulou, E. Golias, P. Tsipas, A. Dimoulas, Appl. Phys. Lett 103 (2013) 231604.
[11] Y. Yuan, R. Quhe, J. Zheng, Y. Wang, Z. Ni, J. Shi, J. Lu, Phys. E 58 (2014) 38.
[12] S. Chahangirov, M. Audiffred, P. Tang, A. Iacomino, W. Duan, G. Merino, A. Rubio, Phys. Rev. B 88 (2013) 035432.
[13] R. Wang, X.D. Pi, Z.Y. Ni, Y. Liu, S.S. Lin, M.S. Xu, D. Yang, Sci. Rep. 3 (2013) 3507.
[14] T. Morishita, M.J.S. Spencer, Sci. Rep 5 (2015) 17570.
[15] Y. Du, J.C. Zhuang, H.S. Liu, X. Xu, S. Eilers, K. Wu, P. Cheng, J.J. Zhao, X.D. Pi, K.W. See, G. Peleckis, X.L. Wang, S.X. Dou, ACS Nano 8 (2014) 10019–10025.
[16] X. Xu, J.C. Zhuang, Y. Du, H.F. Feng, N. Zhang, C. Liu, T. Lei, J. Wang, M. Spencer, T. Morishita, X.L. Wang, S.X. Dou, Sci. Rep. 4 (2014) 7543.
[17] N.W. Johnson, D.I. Muir, A. Moewes, Sci. Rep. 6 (2016) 22510.
[18] P.E. Blochl, Phys. Rev. B 50 (1994) 17953–17979.
[19] G. Kresse, D. Joubert, Phys. Rev. B 59 (1999) 1758–1775.
[20] H. Jia, R. Wang, Z.Y. Ni, Y. Liu, X.D. Pi, D. Yang, J Mater. Sci. Technol 33 (2017) 59–64.
[21] R. Stephan, M.C. Hanf, P. Sonnet, J. Phys. Condens. Matter 27 (2015) 015002.
[22] H.J. Monkhorst, J.D. Pack, Phys. Rev. B 13 (1976) 5188–5192.
[23] R.F.W. Bader, Chem. Rev. 5 (1991) 893–928.
[24] G. Henkelman, A. Arnaldsson, H. Jonsson, Comp. Mater. Sci 36 (2006) 354–360.
[25] C.L. Lin, R. Arafune, K. Kawahara, M. Kanno, N. Tsukahara, E. Minamitani, Y. Kim, M. Kawai, N. Takagi, Phys. Rev. Lett. 110 (2013) 076801.
[26] Z.X. Guo, A. Oshiyama, Phys. Rev. B 89 (2014) 155418.
[27] Z.X. Guo, S. Furuya, J.I. Iwata, A. Oshiyama, Phys. Rev. B 87 (2013) 235435.
[28] Z.X. Guo, S. Furuya, J.I. Iwata, A. Oshiyama, J. Phys. Soc. Jpn 82 (2013) 063714.
[29] P. Kaghazchi, T. Jacob, Phys. Rev. B 81 (2010) 075431.
[30] K. Reuter, M. Scheffler, Phys. Rev. B 65 (2001) 035406.
[31] D.R. Stull, H. Prophet, JANAF Thermochemical Tables, second ed., U.S. National Bureau of Standards, EPO, U.S., Washington DC, 1971.
[32] G. Job, F. Herrmann, Eur. J. Phys. 27 (2006) 353.
[33] M.R. Tchalala, H. Enriquez, H. Yildirim, A. Kara, A.J. Mayne, G. Dujardin, M.A. Ali, H. Oughaddou, Appl. Surf. Sci. 303 (2014) 61–66.
[34] T. Morishita, M.J.S. Spencer, S. Kawamoto, I.K. Snook, J. Phys. Chem. C 117 (2013) 22142.
[35] A. Allred, J. Inorg. Nucl. Chem 17 (1961) 215.
[36] A.K. Singh, V. Kumar, Y. Kawazoe, Phys. Rev. B 7 (2005) 155422.